

## Supporting Information

### Bandgap bowing in a zero-dimensional hybrid halide perovskite derivative: spin-orbit coupling versus lattice strain†

Soumyo Chatterjee,<sup>1</sup> Julia Payne,<sup>2</sup> John T. S. Irvine,<sup>2</sup> and Amlan J. Pal\*<sup>1</sup>

<sup>1</sup> School of Physical Sciences, Indian Association for the Cultivation of Science, Jadavpur, Kolkata 700032, India

<sup>2</sup> School of Chemistry, University of St Andrews, Scotland KY16 9ST, UK

E-mail: sspajp@iacs.res.in

**Table S1** Unit cell parameters of  $\text{MA}_3(\text{Sb}_{1-x}\text{Bi}_x)_2\text{I}_9$  ( $0 \leq x \leq 1$ ) obtained from XRD patterns fitted using Pawley refinement.

Bi-content ( $x$ ) in $\text{MA}_3(\text{Sb}_{1-x}\text{Bi}_x)_2\text{I}_9$	Lattice parameters		Unit cell volume ( $\text{\AA}^3$ ) <sup>3</sup>
	$a = b$ ( $\text{\AA}$ )	$c$ ( $\text{\AA}$ )	
0.0	8.611(2)	21.458(2)	1378.8(4)
0.1	8.548(1)	21.530(2)	1362.4(4)
0.2	8.559(2)	21.529(3)	1365.9(6)
0.3	8.549(1)	21.547(1)	1363.8(3)
0.4	8.562(2)	21.578(2)	1370.1(5)
0.5	8.545(2)	21.597(2)	1365.9(5)
0.6	8.546(3)	21.620(1)	1368.0(4)
0.7	8.547(2)	21.635(2)	1371.8(7)
0.8	8.573(2)	21.670(2)	1379.4(6)
0.9	8.568(1)	21.704(1)	1383.1(3)
1.0	8.605(2)	21.737(1)	1394.0(4)

**Table S2** Band energies and transport gap of  $\text{MA}_3(\text{Sb}_{1-x}\text{Bi}_x)_2\text{I}_9$  ( $0 \leq x \leq 1$ ) composites obtained from STS measurements and DOS spectra.

Bi-content ( $x$ ) in $\text{MA}_3(\text{Sb}_{1-x}\text{Bi}_x)_2\text{I}_9$	CB-edge (eV)	VB-edge (eV)	Transport gap (eV)
0.0	-1.37	1.23	2.60
0.1	-1.27	1.21	2.48
0.2	-1.18	1.19	2.37
0.3	-1.14	1.16	2.30
0.4	-1.11	1.15	2.26
0.5	-1.09	1.13	2.22
0.6	-1.23	1.19	2.42
0.7	-1.28	1.23	2.51
0.8	-1.30	1.24	2.54
0.9	-1.33	1.24	2.57
1.0	-1.34	1.25	2.59

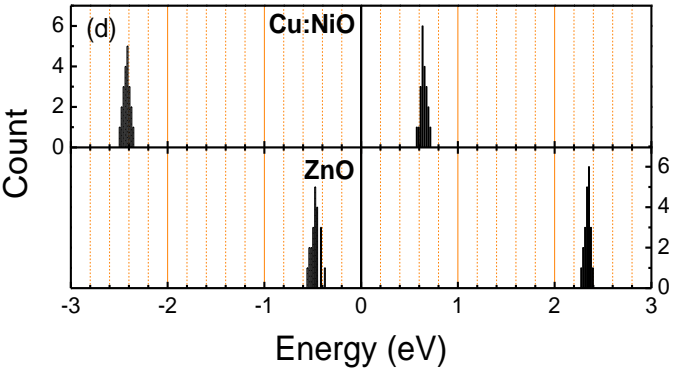
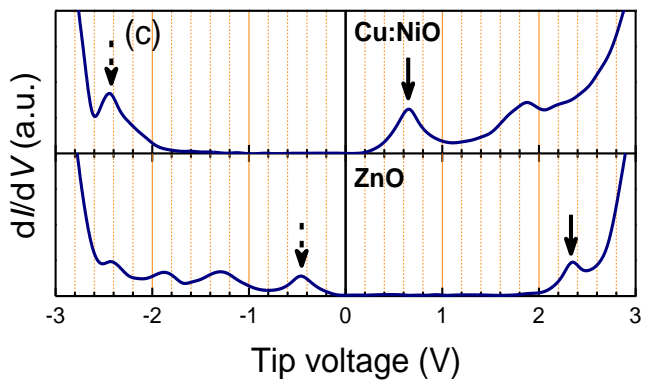
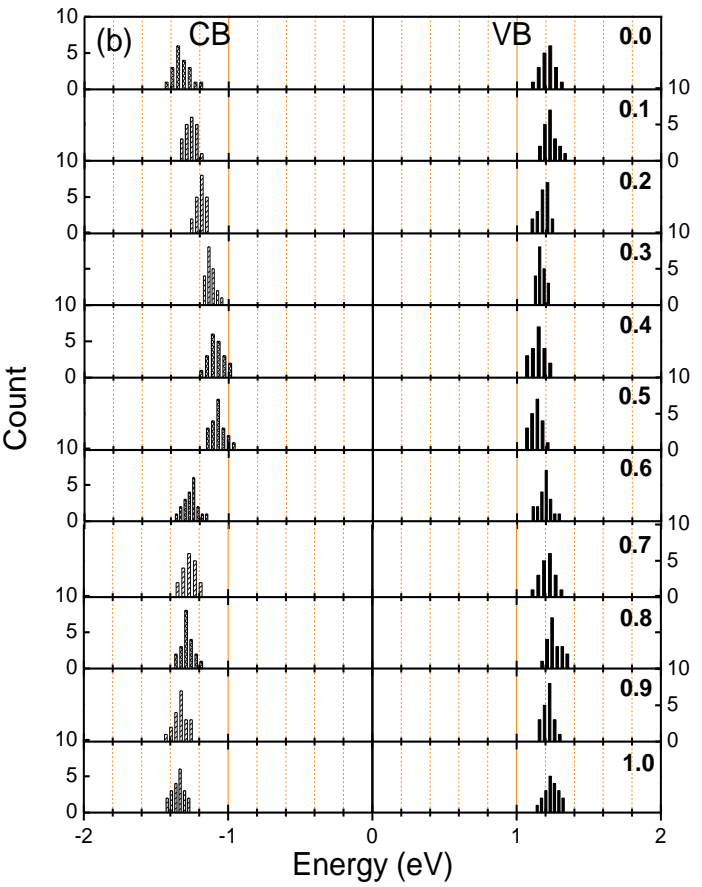
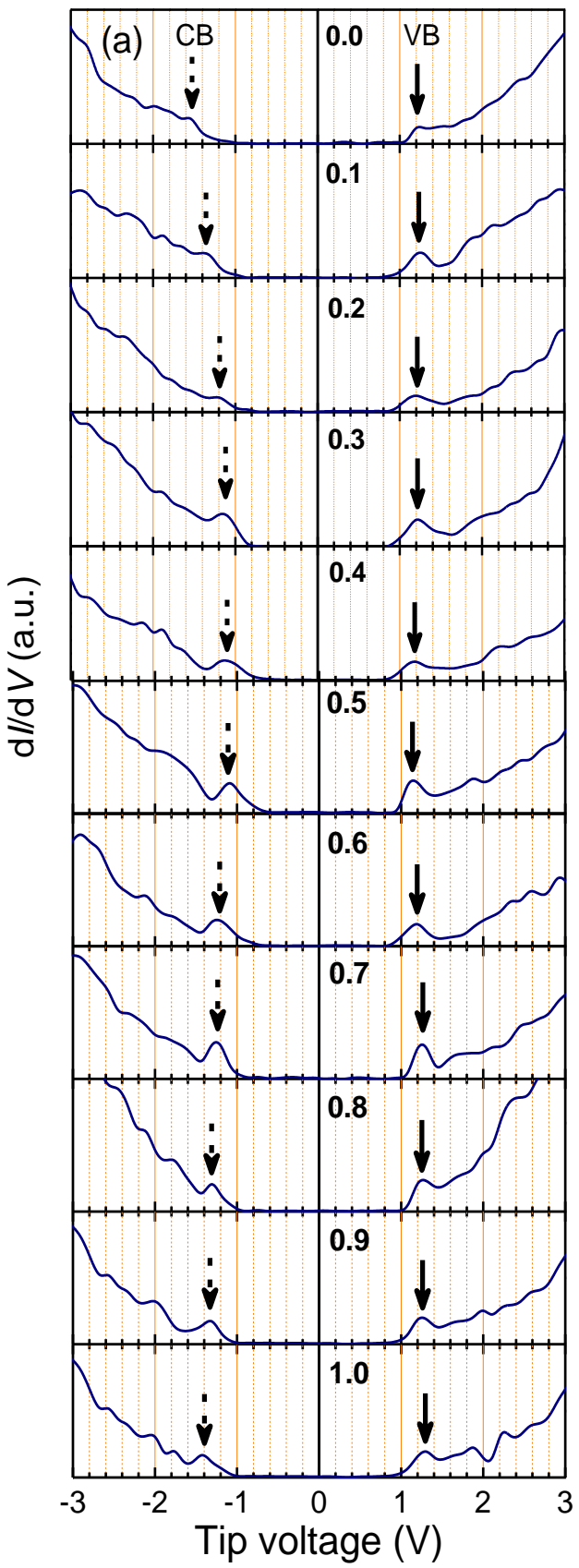


**Fig. S1** (a)  $dI/dV$  versus tip voltage plots of  $MA_3(Sb_{1-x}Bi_x)_2I_9$  thin-films with different bismuth-content ( $x$ ) as stated in the legends, and (b) respective histogram of CB and VB edges, (c) and (d) present  $dI/dV$  versus tip voltage plots and histogram of CB and VB edges of Cu:NiO and ZnO carrier selective contacts, respectively.

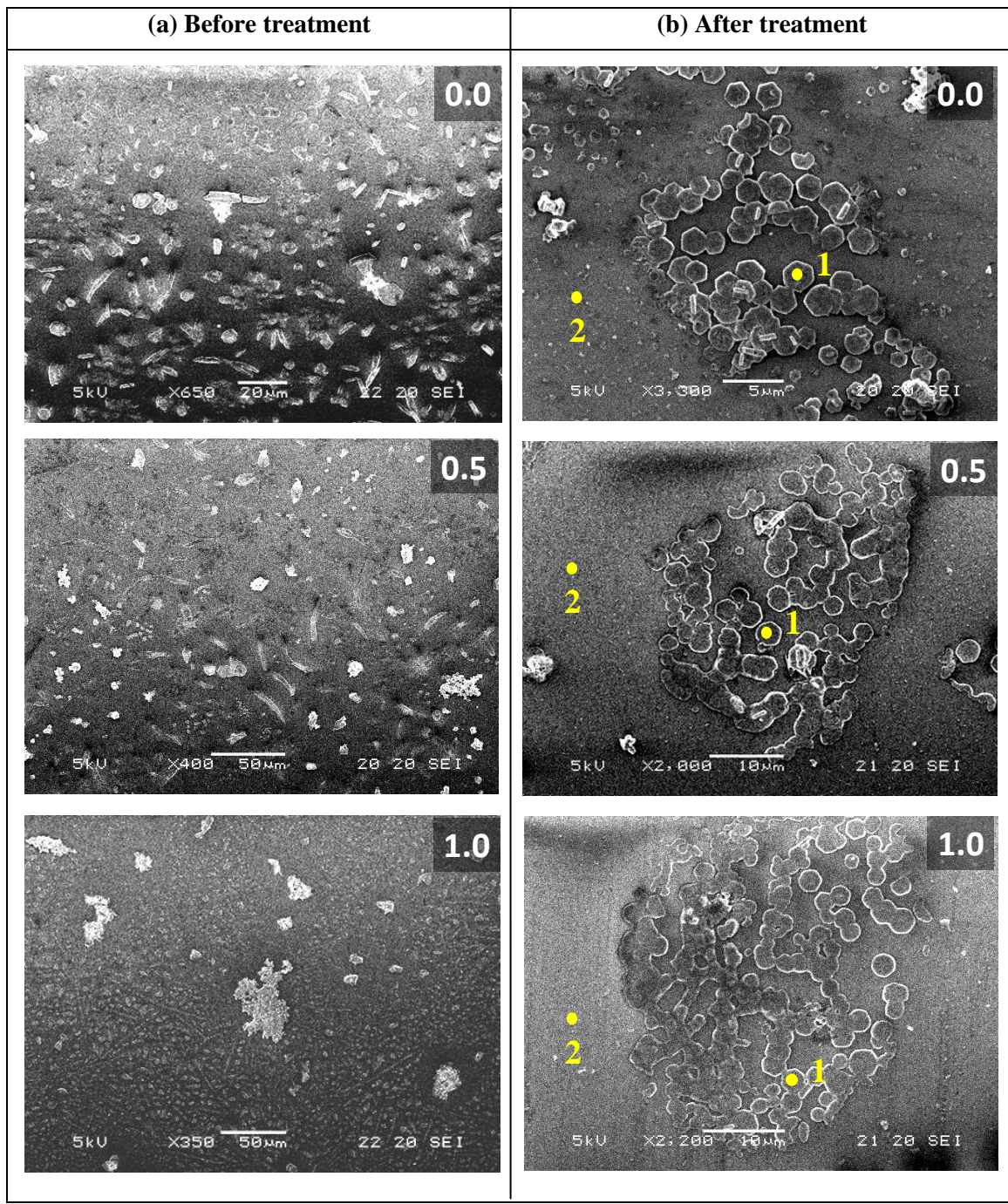


**Fig. S2** SEM images of  $\text{MA}_3(\text{Sb}_{1-x}\text{Bi}_x)_2\text{I}_9$  films having bismuth-content ( $x$ ) as specified in the legends (a) before and (b) after chlorobenzene treatment. The points of EDX measurement have been marked with yellow dots and numbers.

**Table S3** Distribution (atomic %) of individual elements observed on particular spots of  $\text{MA}_3(\text{Sb}_{1-x}\text{Bi}_x)_2\text{I}_9$  thin-films having specified bismuth-content ( $x$ ).

Bi-content ( $x$ ) in $\text{MA}_3(\text{Sb}_{1-x}\text{Bi}_x)_2\text{I}_9$	Position	Elements			Ratio	
		Sb L	Bi M	I L	Sb/Bi	I/(Bi+Sb)
<b>0.0</b>	Point 1: Hexagon	0.0	22.2	77.8	—	3.6
	Point 2: Film	0.0	6.3	93.7	—	14.3
<b>0.5</b>	Point 1: Hexagon	10.4	11.5	78.1	0.9	3.6
	Point 2: Film	3.5	5.4	91.1	0.6	10.0
<b>1.0</b>	Point 1: Hexagon	21.5	0.0	78.5	—	3.7
	Point 2: Film	13.9	0.0	86.1	—	6.2

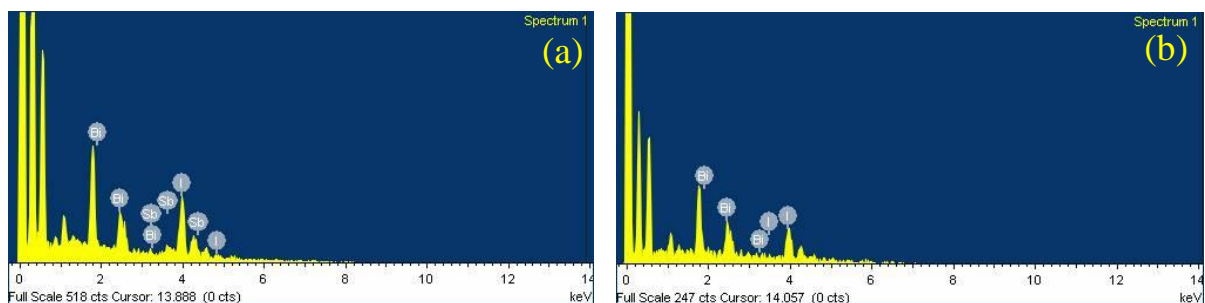


**Fig. S3** EDX spectra of  $\text{MA}_3(\text{Sb}_{0.5}\text{Bi}_{0.5})_2\text{I}_9$  thin-films taken on the (a) Point 1: hexagon and (b) Point 2: film, respectively.

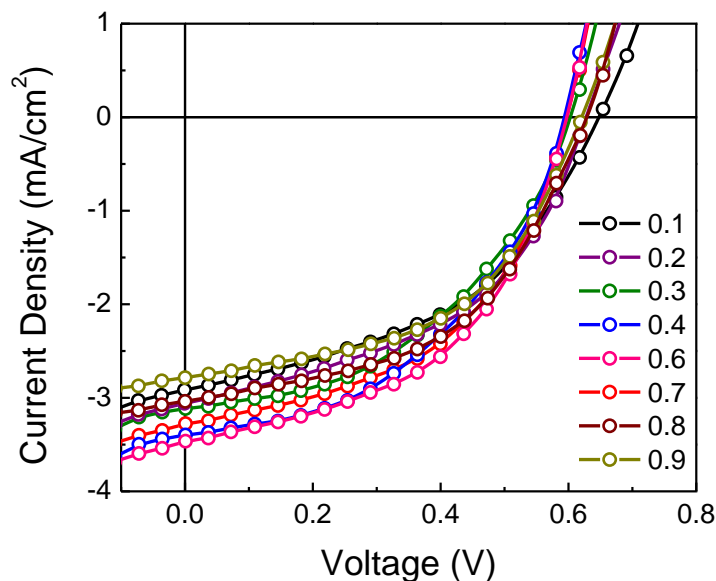


**Fig. S4** Current-voltage characteristics of  $\text{MA}_3(\text{Sb}_{1-x}\text{Bi}_x)_2\text{I}_9$  with bismuth-contents ( $x$ ) as specified in the legends (under 1 sun illumination).